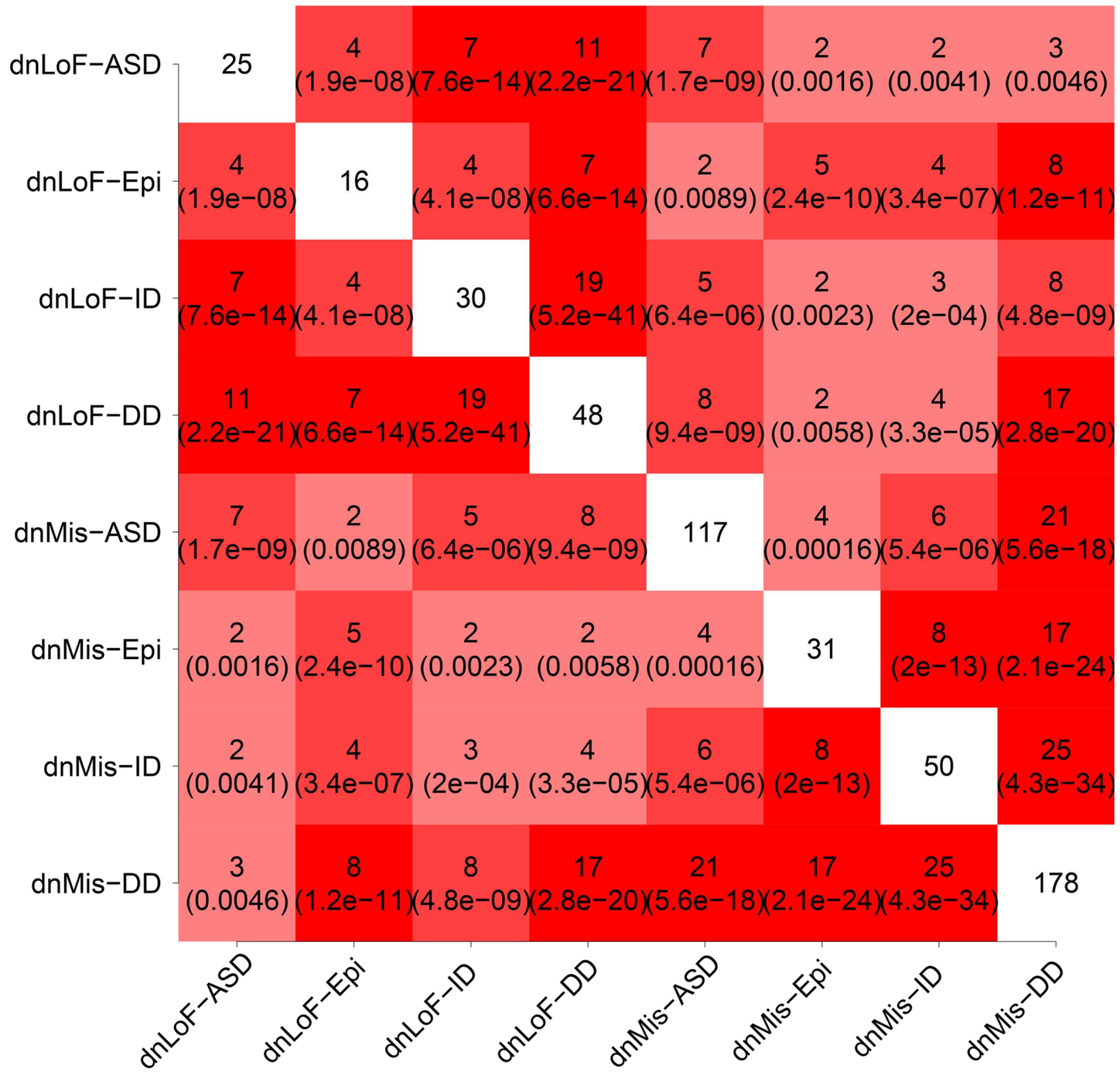

Supplemental Figure S1. Overlap between eight NDD gene sets. Square matrix shows the number of overlapping genes between two NDD gene sets and the associated statistical significance P value calculated by the one-sided Fisher's exact test.

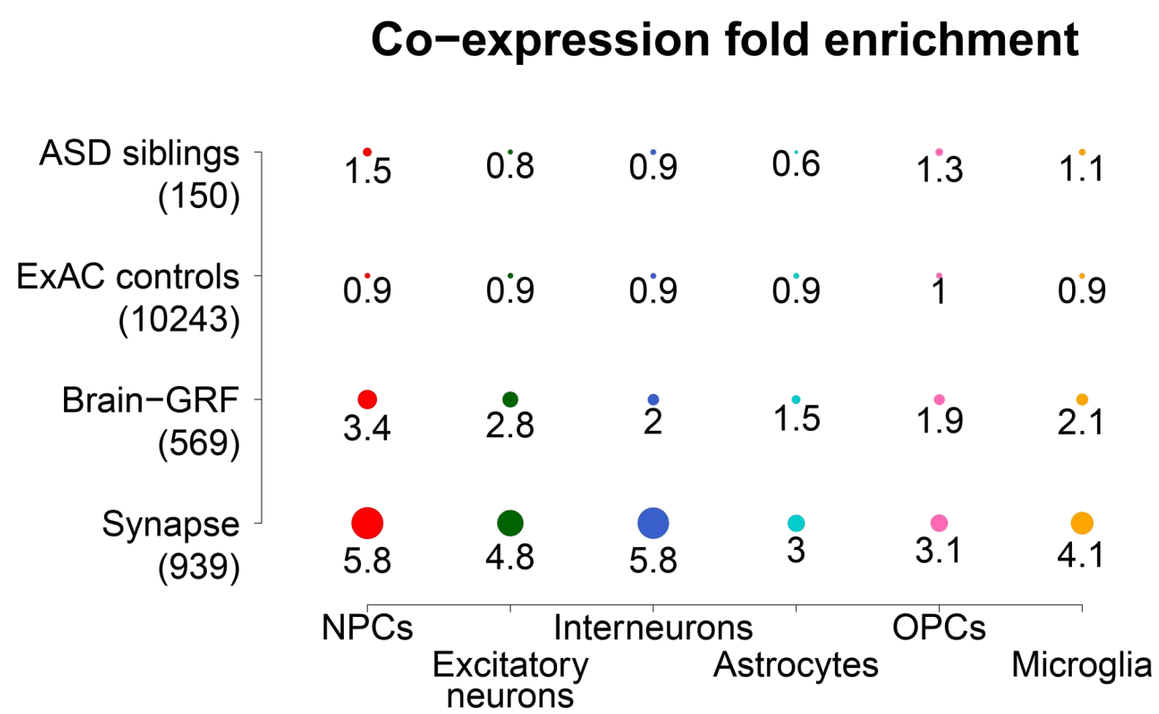

Supplemental Figure S2. Control gene sets show low co-expression enrichment in six major cell types. Co-expression fold enrichment of four control gene sets in six major cell types. Gene set size is shown in parentheses. Circle size is proportional to co-expression fold enrichment score.

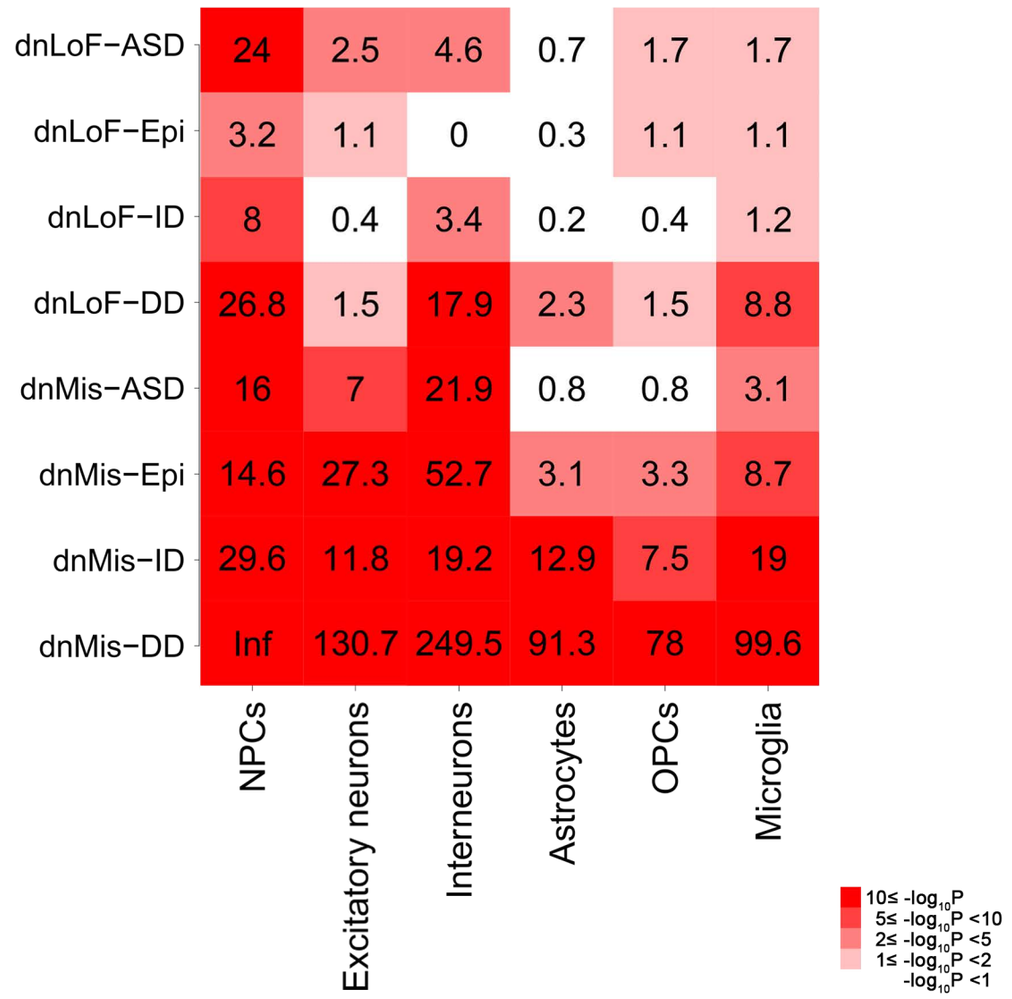

Supplemental Figure S3. Significance values of co-expression enrichment analysis of eight NDD gene sets compared with the background genes. $-\log_{10}P$ value in rectangular matrix indicates whether the NDD gene set in the corresponding row has a higher co-expression fold enrichment score than the background genes of the cell type in the corresponding column by the one-sided Fisher's exact test.

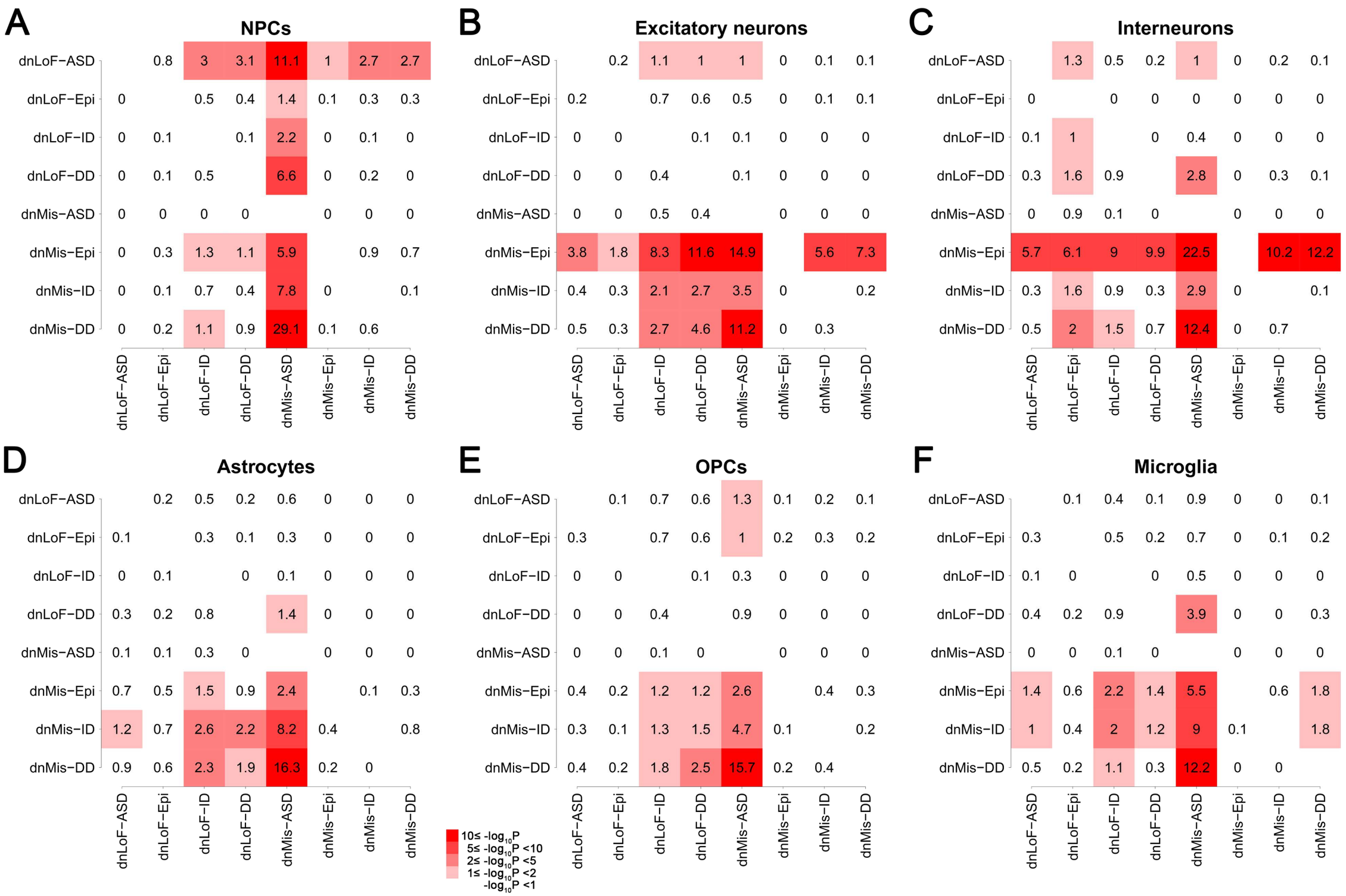

Supplemental Figure S4. Significance values of pairwise co-expression fold enrichment comparison between eight NDD gene sets. (*A-F*) Square matrix shows significance values of pairwise co-expression fold enrichment comparison between eight NDD gene sets in NPCs (*A*), excitatory neurons (*B*), interneurons (*C*), astrocytes (*D*), OPCs (*E*), and microglia (*F*). -$\log_{10}$P value in each square matrix indicates whether the NDD gene set in the corresponding row has a higher co-expression fold enrichment score than the NDD gene set in the corresponding column by the one-sided Fisher's exact test.

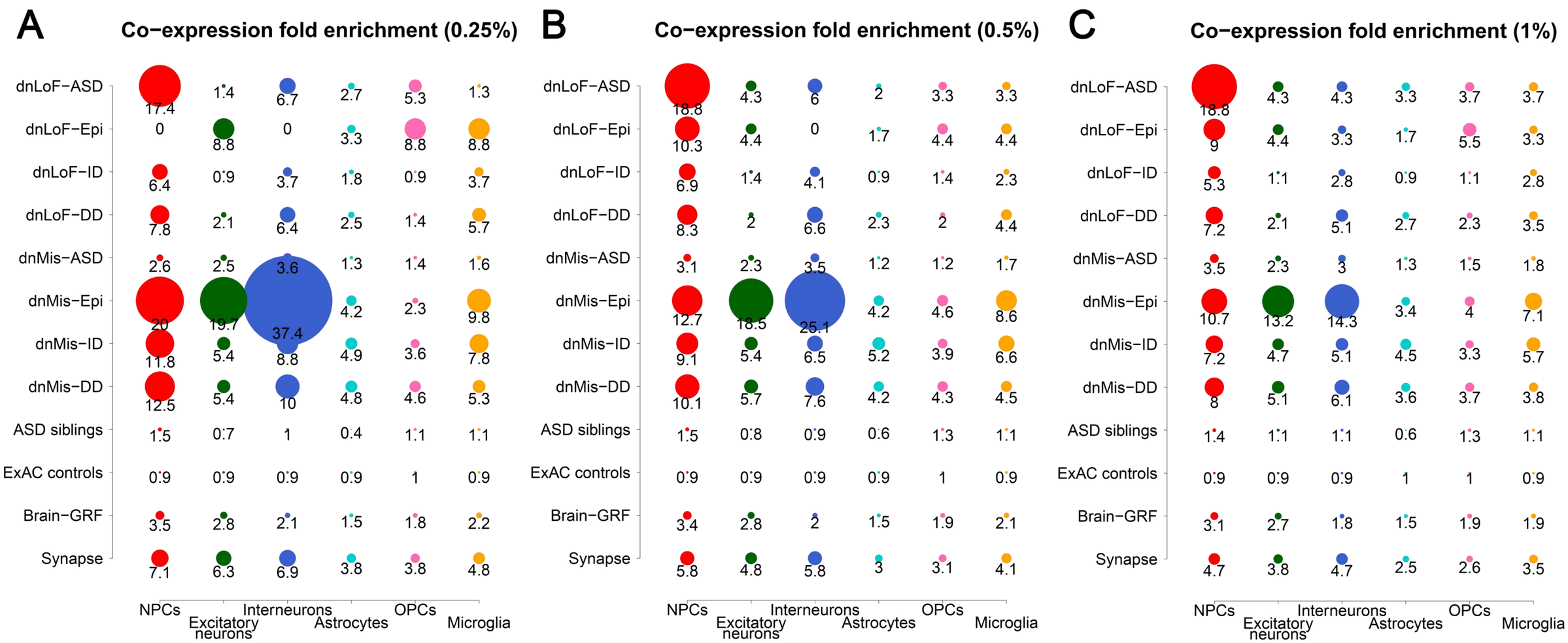

Supplemental Figure S5. Co-expression enrichment analysis of twelve gene sets in six major cell types at different co-expression thresholds. (*A*-*C*) Co-expression fold enrichment of eight NDD gene sets and four control gene sets in six major cell types at co-expression thresholds of top 0.25% (*A*), top 0.5% (*B*), and top 1% (*C*). Circle size is proportional to co-expression fold enrichment score.

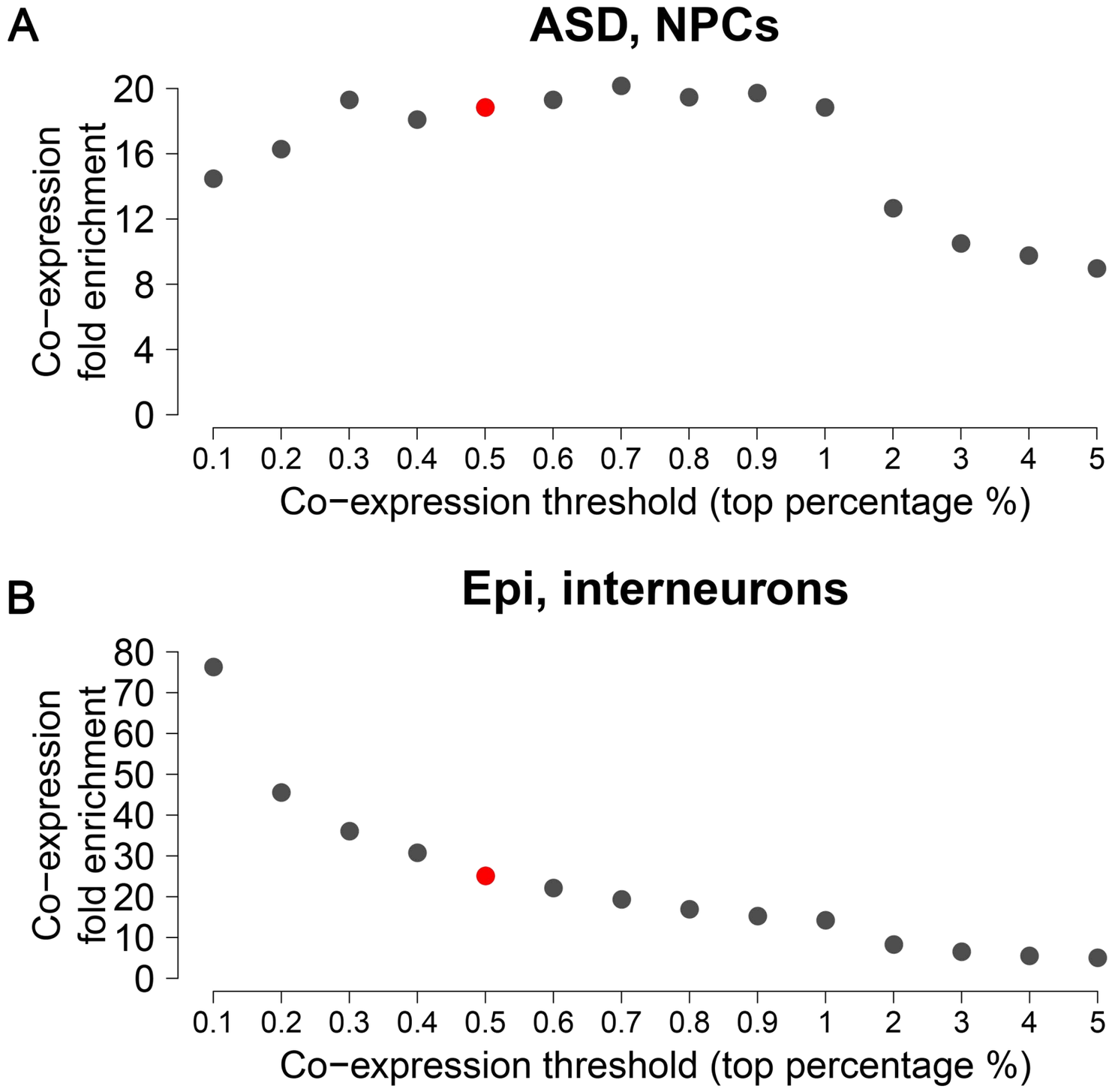

Supplemental Figure S6. Co-expression enrichment analysis of dnLoF-ASD genes in NPCs and dnMis-Epi genes in interneurons at varying co-expression thresholds. (*A,B*) Co-expression fold enrichment of dnLoF-ASD genes in NPCs (*A*) and dnMis-Epi genes in interneurons (*B*) at varying co-expression thresholds between top 0.1% and top 5%.

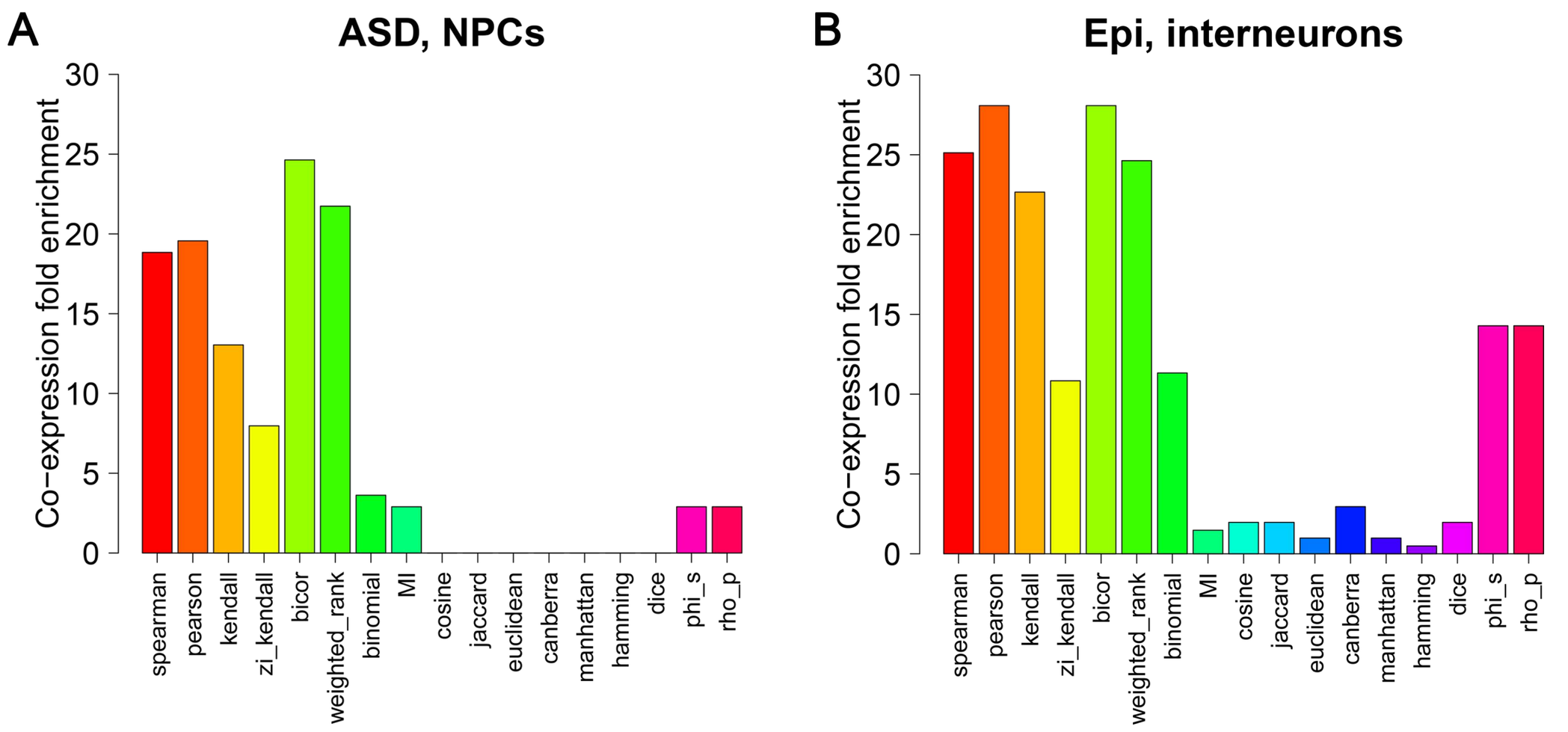

Supplemental Figure S7. Co-expression enrichment analysis of dnLoF-ASD genes in NPCs and dnMis-Epi genes in interneurons using different measures of association. (*A,B*) Co-expression fold enrichment of dnLoF-ASD genes in NPCs (*A*) and dnMis-Epi genes in interneurons (*B*) using 17 measures of association implemented in the 'dismay' R package.

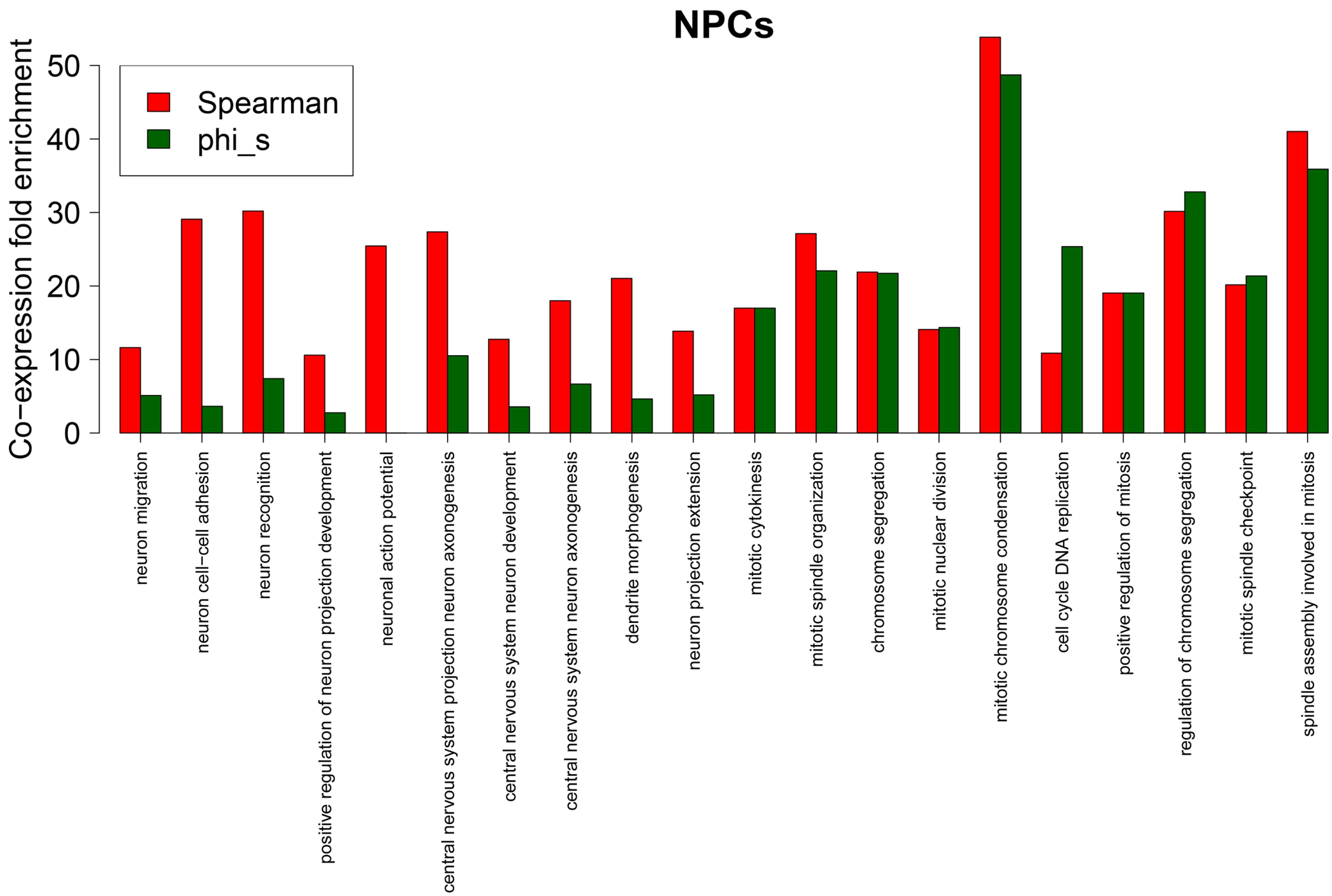

Supplemental Figure S8. Co-expression fold enrichment scores of the representative GO biological process terms in NPCs calculated using Spearman's correlation and proportionality phi_s. Co-expression fold enrichment scores calculated using Spearman's correlation can capture both neuron developmental pathways and cell cycle-related processes which are known to be highly correlated during NPC development.

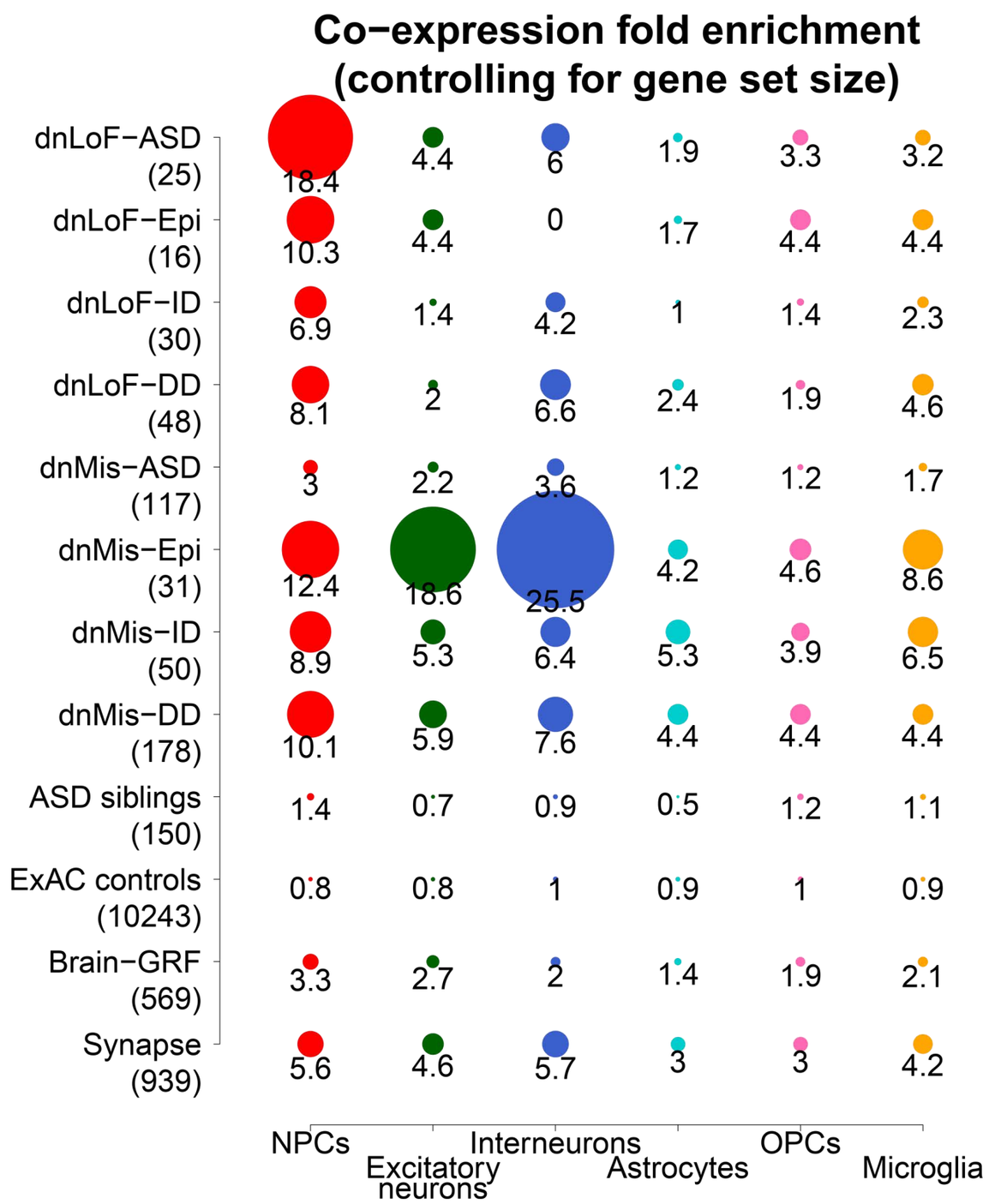

Supplemental Figure S9. Co-expression enrichment analysis of twelve gene sets in six major cell types by controlling for gene set size. For all the twelve gene sets in each cell type, co-expression enrichment score is computed using randomly chosen twelve gene sets with the same gene set size (the minimum gene set size of the original twelve gene sets in the cell type) from the original twelve gene sets 1000 times. Gene set size is shown in parentheses. Circle size is proportional to co-expression fold enrichment score.

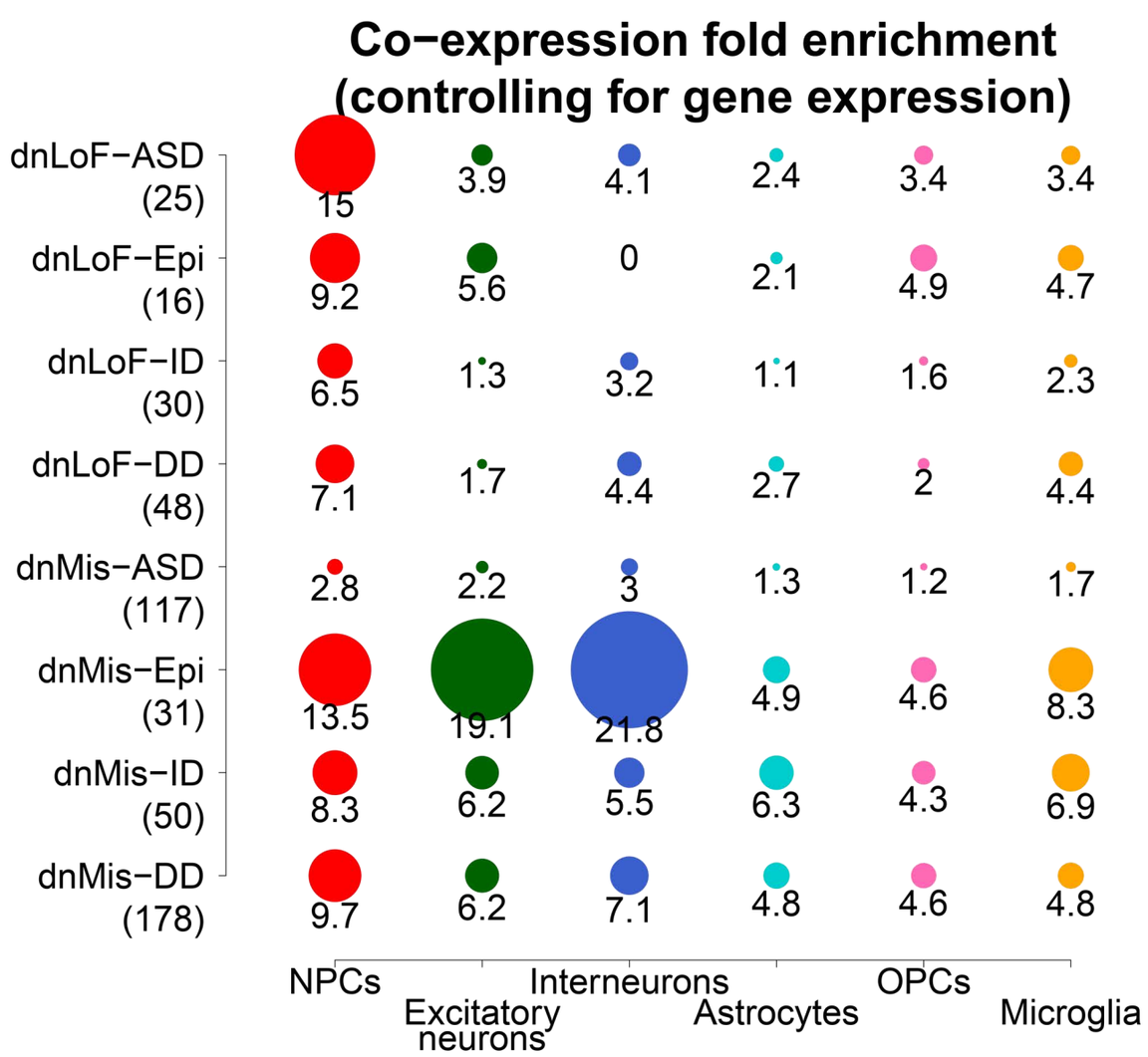

Supplemental Figure S10. Co-expression enrichment analysis of eight NDD gene sets in six major cell types by controlling for expression level dependence. For each gene set in each cell type, co-expression enrichment score is computed using 1000 randomly chosen gene sets with similar expression levels in the cell type as the background gene set. Gene set size is shown in parentheses. Circle size is proportional to co-expression fold enrichment score.

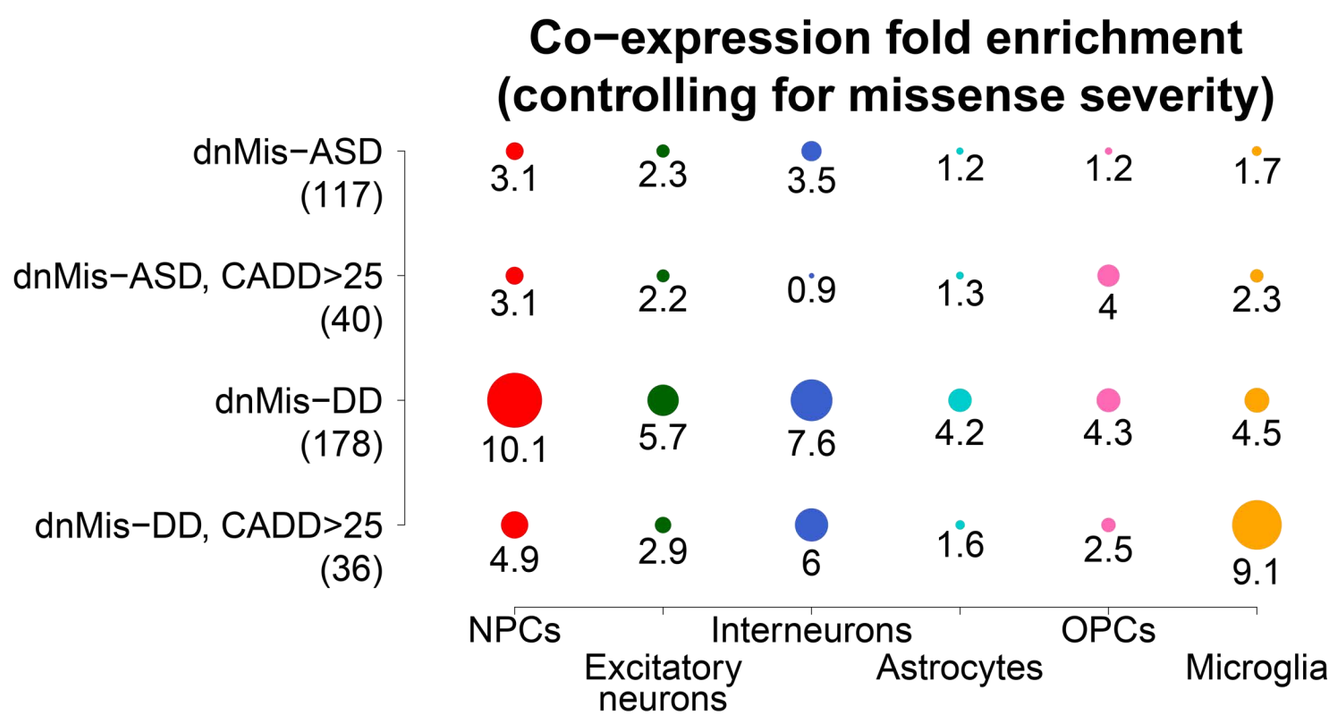

Supplemental Figure S11. Co-expression enrichment analysis of ASD and DD gene sets with dnMis mutations in six major cell types by controlling for missense severity. Co-expression fold enrichment of ASD and DD gene sets with dnMis mutations and those with severe dnMis mutations (CADD score>25) in six major cell types. Gene set size is shown in parentheses. Circle size is proportional to co-expression fold enrichment score.

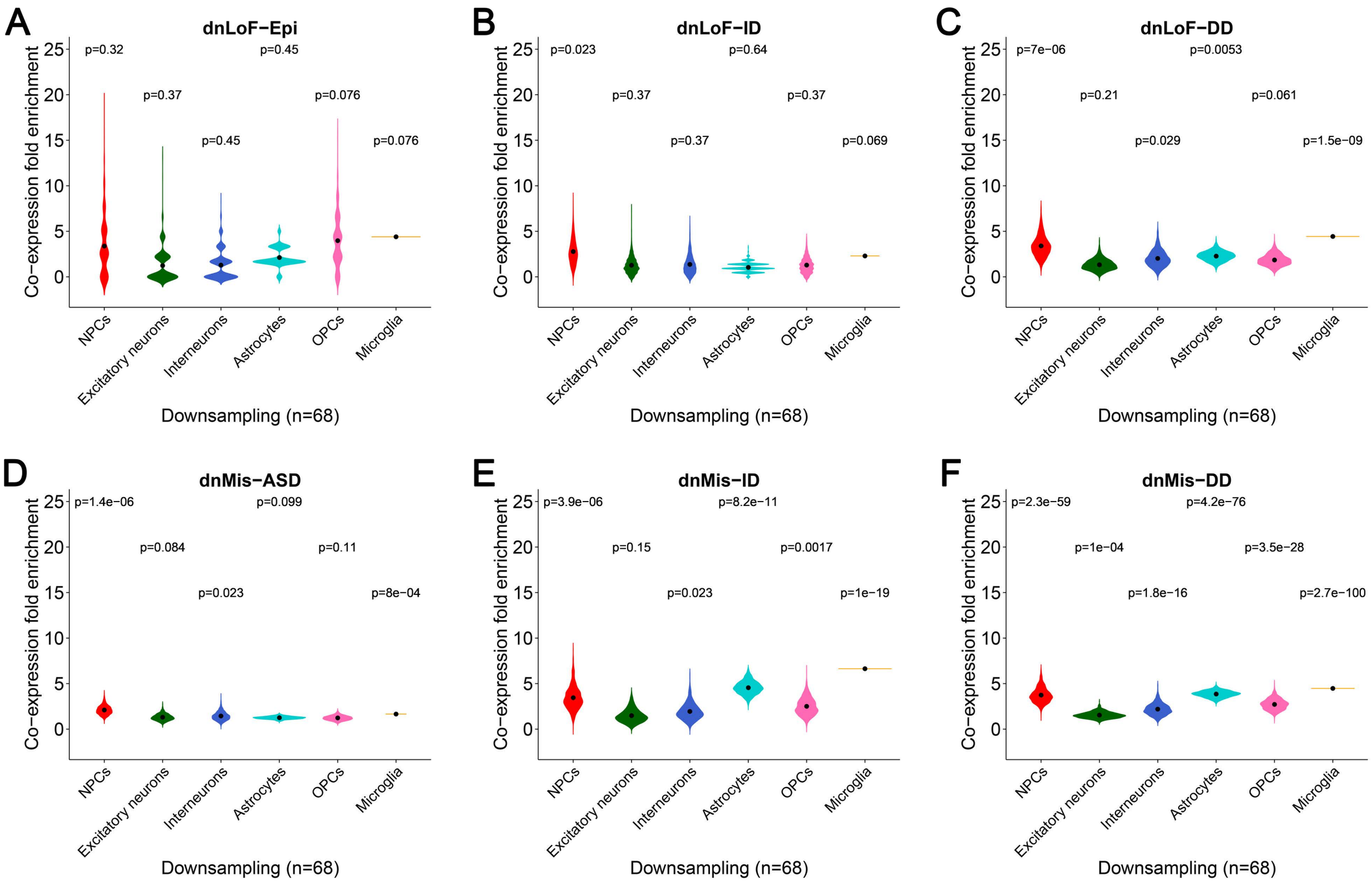

Supplemental Figure S12. Co-expression enrichment analysis of the other six NDD gene sets in six major cell types by downsampling. (*A-F*) Co-expression fold enrichment of dnLoF-Epi (*A*), dnLoF-ID (*B*), dnLoF-DD (*C*), dnMis-ASD (*D*), dnMis-ID (*E*), and dnMis-DD genes (*F*) in six major cell types by downsampling the same number of cells for each cell type. Violin plot shows the mean value (point). P value indicates whether the mean co-expression fold enrichment score of the corresponding gene set is higher than that of the background genes (one-sided Fisher's exact test).

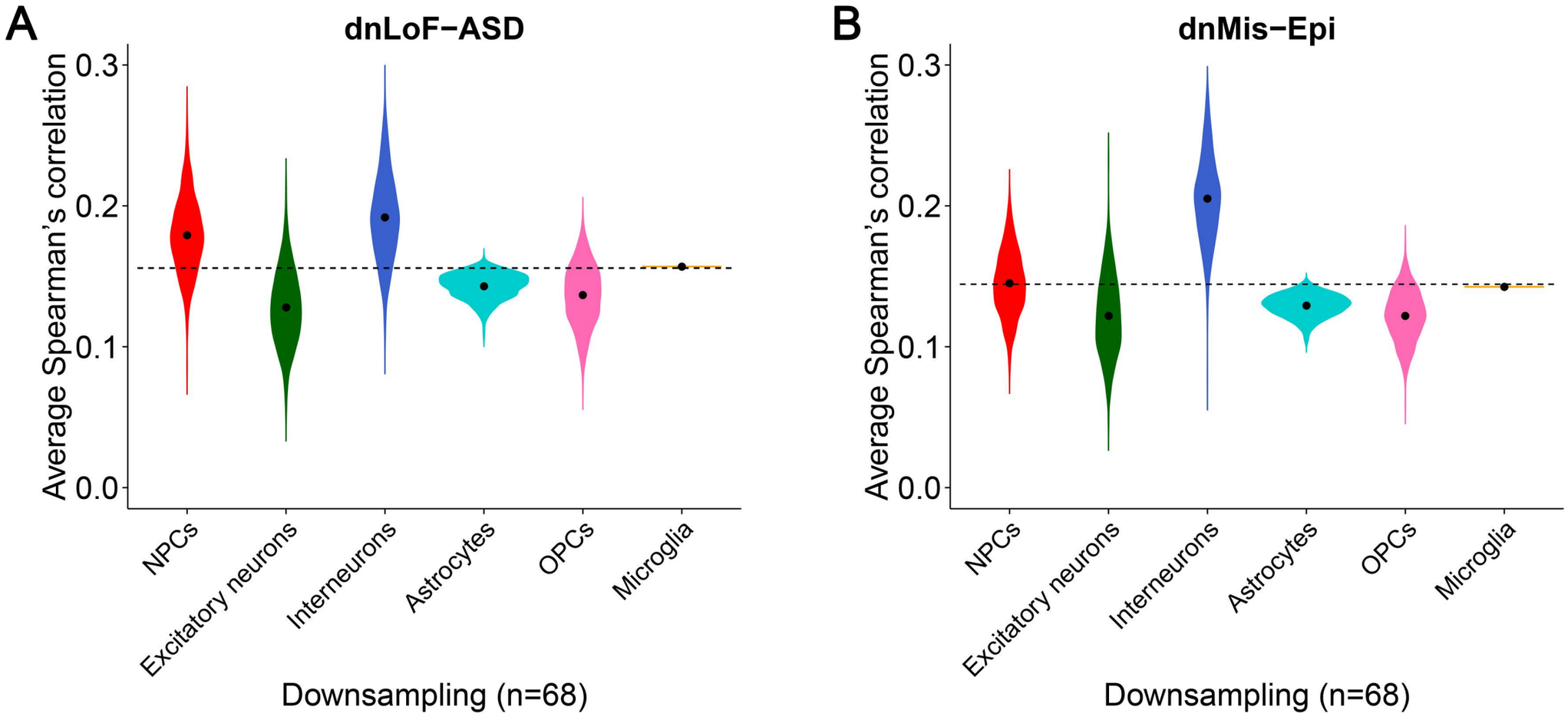

Supplemental Figure S13. Spearman's correlation analysis of dnLoF-ASD and dnMis-Epi genes in six major cell types by downsampling. (*A,B*) Average Spearman's correlation of dnLoF-ASD (*A*) and dnMis-Epi genes (*B*) in six major cell types by downsampling the same number of cells for each cell type. Violin plot shows the mean value (point). Dashed horizontal line indicates the mean of six mean values of 1000 average Spearman's correlation coefficients of an NDD gene set for six major cell types by downsampling.

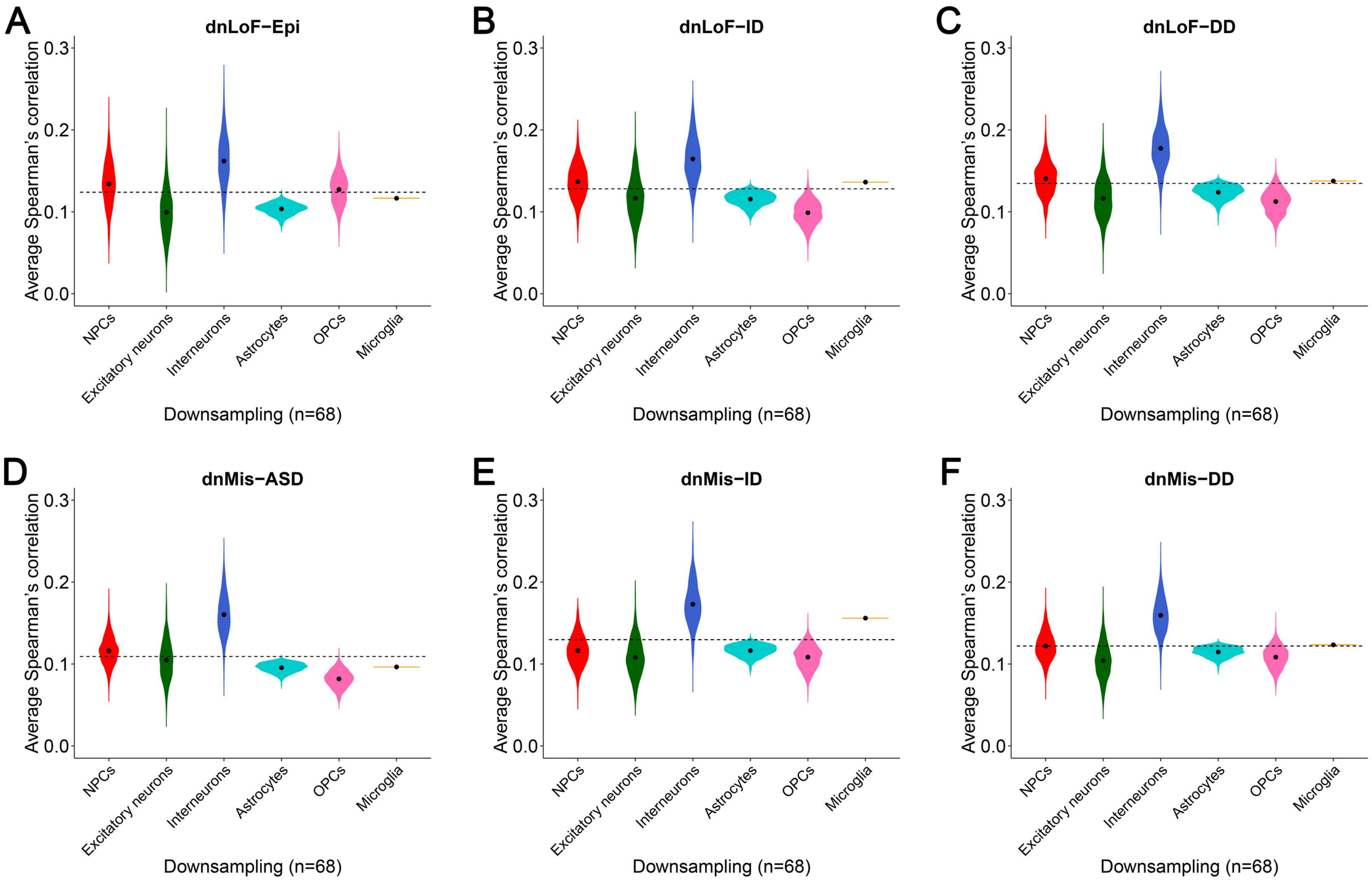

Supplemental Figure S14. Spearman's correlation analysis of the other six NDD gene sets in six major cell types by downsampling. (*A-F*) Average Spearman's correlation of dnLoF-Epi (*A*), dnLoF-ID (*B*), dnLoF-DD (*C*), dnMis-ASD (*D*), dnMis-ID (*E*), and dnMis-DD genes (*F*) in six major cell types by downsampling the same number of cells for each cell type. Violin plot shows the mean value (point). Dashed horizontal line indicates the mean of six mean values of 1000 average Spearman's correlation coefficients of an NDD gene set for six major cell types by downsampling.

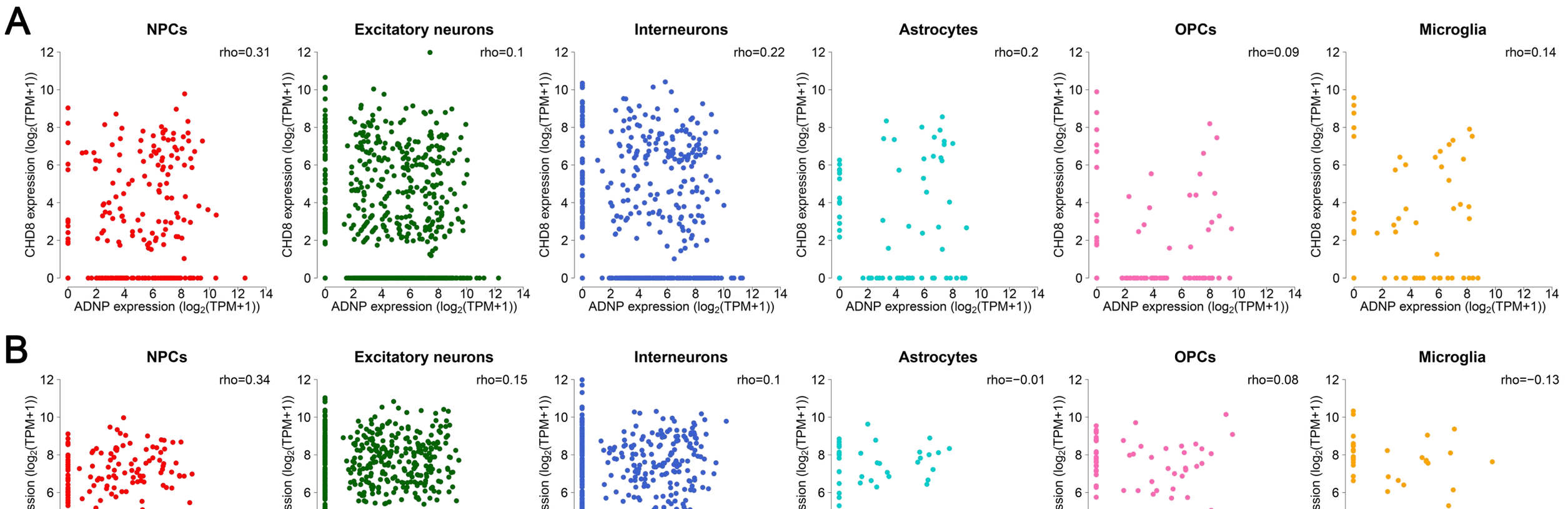

Supplemental Figure S15. Examples of dnLoF-ASD gene pairs that show higher co-expression in NPCs than in the other five major cell types. (*A-D*) Scatter plots show the expression levels of one dnLoF-ASD gene versus the expression levels of another dnLoF-ASD gene in six major cell types. The mean values of 1000 Spearman's correlation coefficients by downsampling are shown.

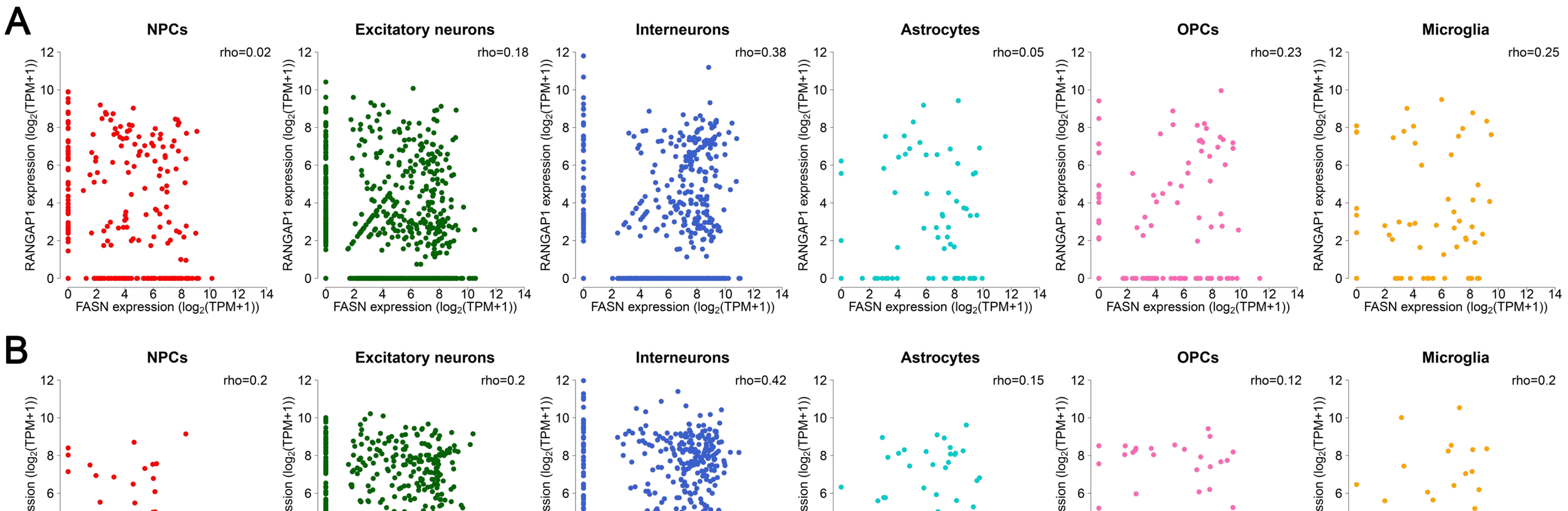

Supplemental Figure S16. Examples of dnMis-Epi gene pairs that show higher co-expression in interneurons than in the other five major cell types. (*A-D*) Scatter plots show the expression levels of one dnMis-Epi gene versus the expression levels of another dnMis-Epi gene in six major cell types. The mean values of 1000 Spearman's correlation coefficients by downsampling are shown.

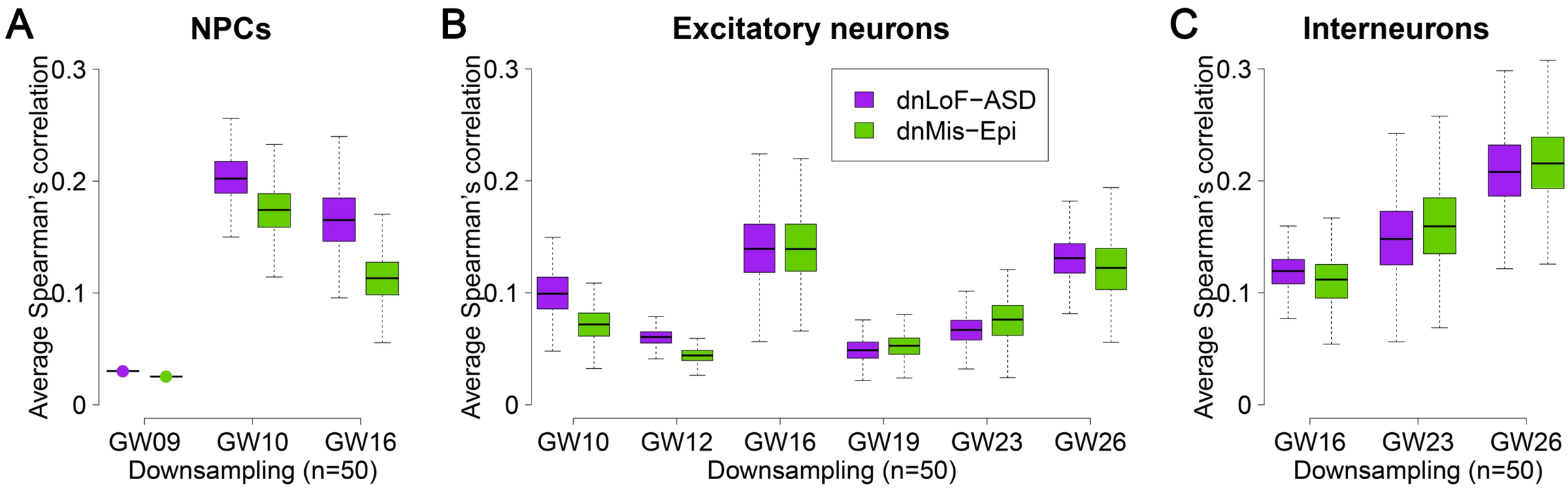

Supplemental Figure S17. Spearman's correlation analysis of dnLoF-ASD and dnMis-Epi genes during NPC and neuron development by downsampling. (*A*-*C*) Average Spearman's correlation of dnLoF-ASD and dnMis-Epi genes at specific stages of NPCs (*A*), excitatory neurons (*B*), and interneurons (*C*) by downsampling the same number of cells for each cell stage.

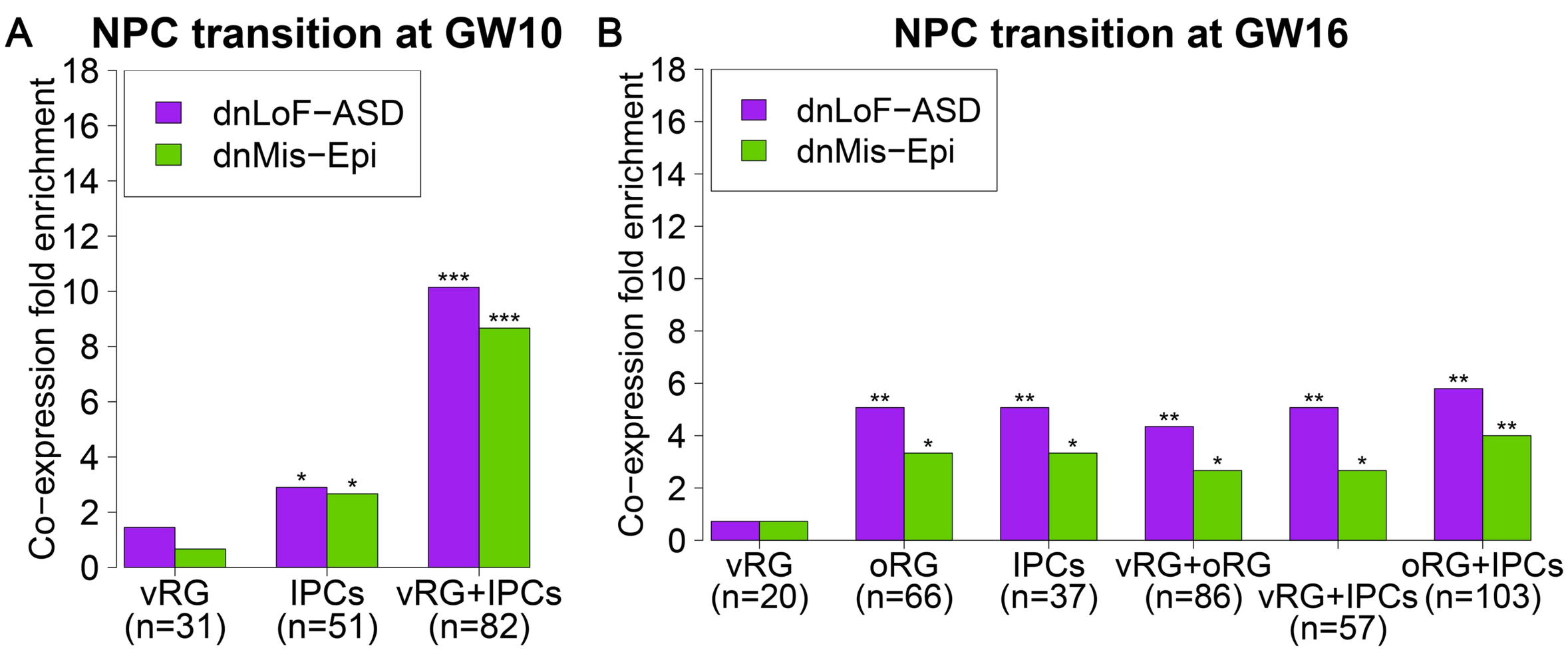

Supplemental Figure S18. Co-expression enrichment analysis of dnLoF-ASD and dnMis-Epi genes during NPC transitions. (*A*) Co-expression fold enrichment of dnLoF-ASD and dnMis-Epi genes in vRG cells, IPCs, and the transition at GW10 using the original number of cells which is shown in parentheses. (*B*) Co-expression fold enrichment of dnLoF-ASD and dnMis-Epi genes in vRG cells, oRG cells, IPCs, and their transitions at GW16 using the original number of cells which is shown in parentheses. In (*A,B*), asterisks indicate $-\log_{10}P$ values for differences in enrichment scores between the gene sets and the background genes (one-sided Fisher's exact test): * $1 \leq -\log_{10}P < 2$; ** $2 \leq -\log_{10}P < 5$; *** $5 \leq -\log_{10}P < 10$; **** $10 \leq -\log_{10}P$.

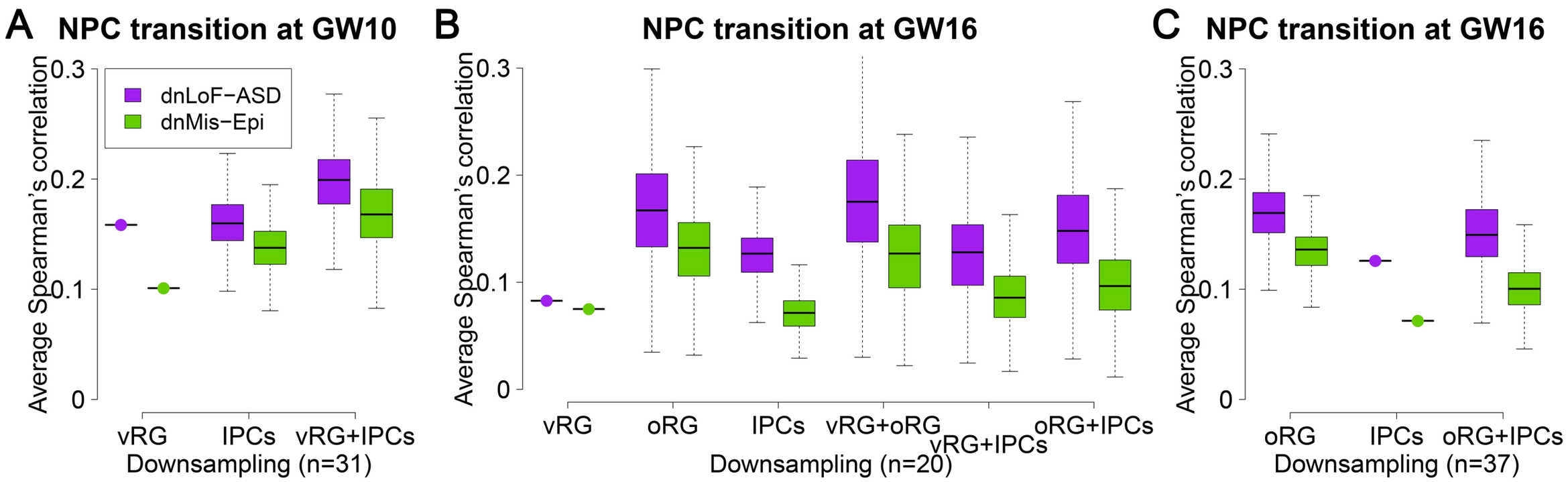

Supplemental Figure S19. Spearman's correlation analysis of dnLoF-ASD and dnMis-Epi genes during NPC transitions by downsampling. (*A*) Average Spearman's correlation of dnLoF-ASD and dnMis-Epi genes in vRG cells, IPCs, and the transition at GW10 by downsampling the same number of cells for each condition. (*B*) Average Spearman's correlation of dnLoF-ASD and dnMis-Epi genes in vRG cells, oRG cells, IPCs, and their transitions at GW16 by downsampling the same number of cells for each condition. (*C*) Average Spearman's correlation of dnLoF-ASD and dnMis-Epi genes in oRG cells, IPCs, and the transition at GW16 by downsampling the same number of cells for each condition.

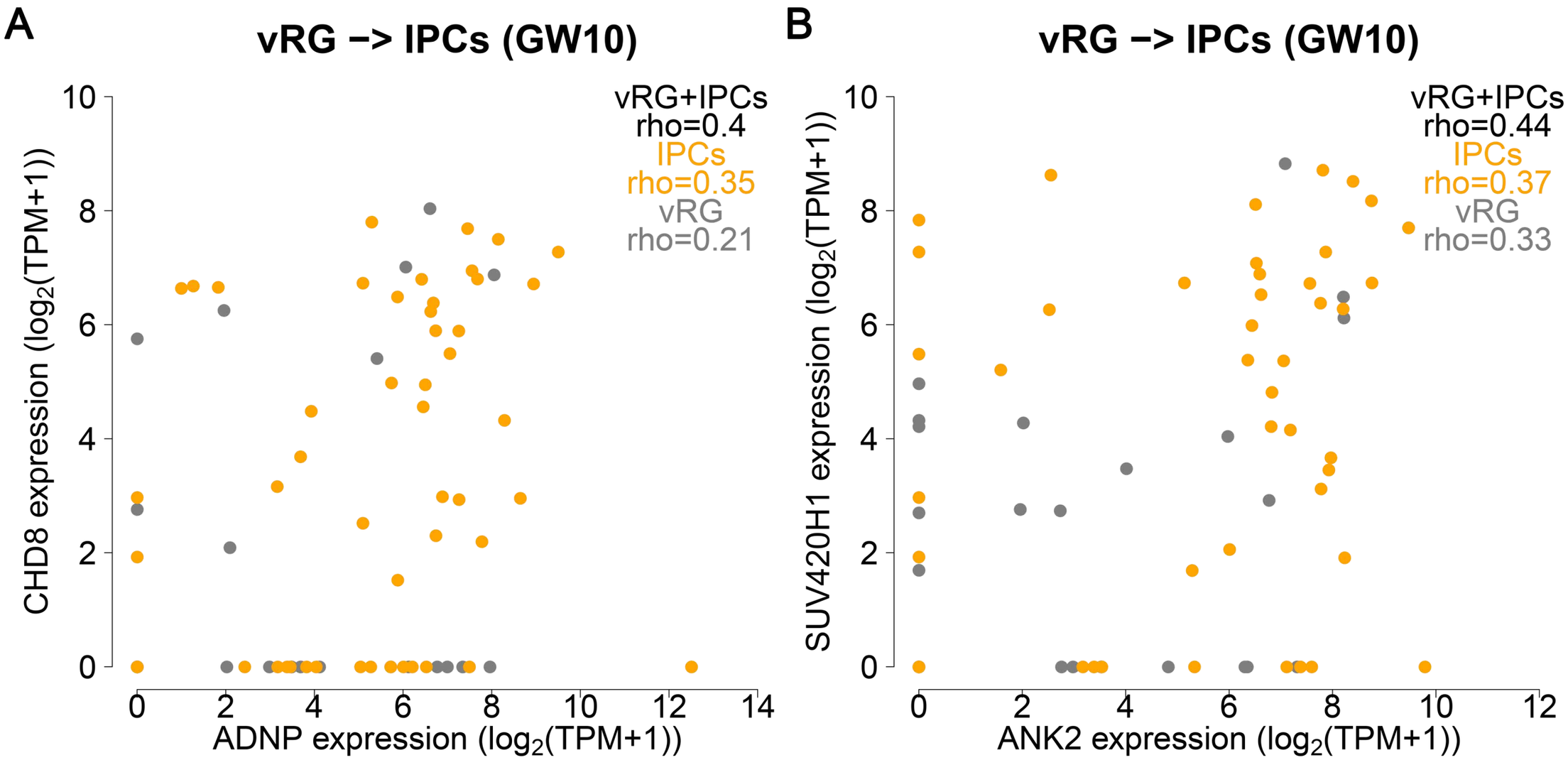

Supplemental Figure S20. Examples of dnLoF-ASD gene pairs that show increased co-expression during the vRG-to-IPC transition at GW10 (vRG cells and IPCs combined) compared with vRG cells or IPCs alone. (*A-D*) Scatter plot shows the expression levels of one dnLoF-ASD gene versus the expression levels of another dnLoF-ASD gene. The mean value of 1000 Spearman's correlation coefficients by downsampling is shown.

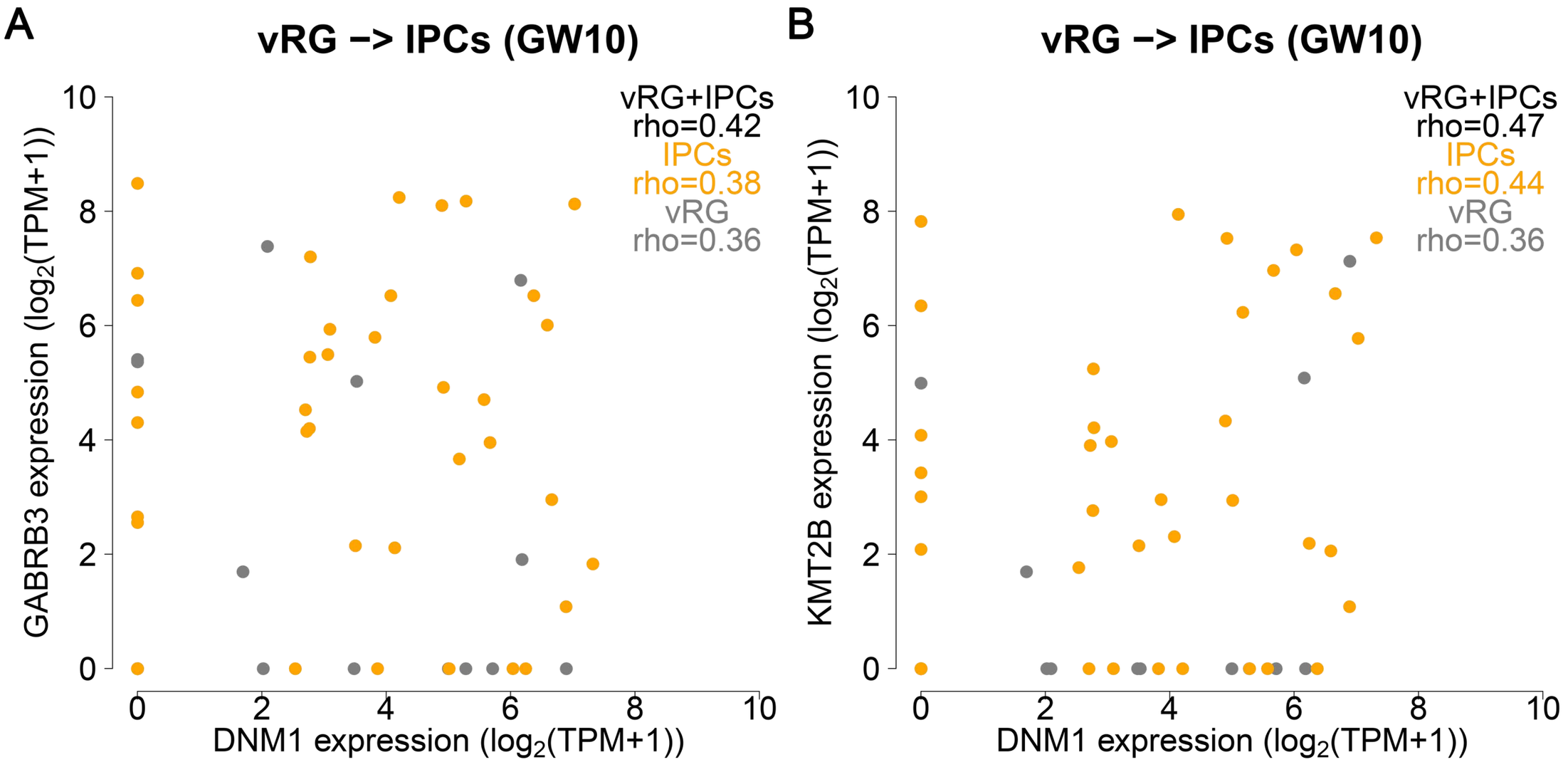

Supplemental Figure S21. Examples of dnMis-Epi gene pairs that show increased co-expression during the vRG-to-IPC transition at GW10 (vRG cells and IPCs combined) compared with vRG cells or IPCs alone. (*A-D*) Scatter plot shows the expression levels of one dnMis-Epi gene versus the expression levels of another dnMis-Epi gene. The mean value of 1000 Spearman's correlation coefficients by downsampling is shown.

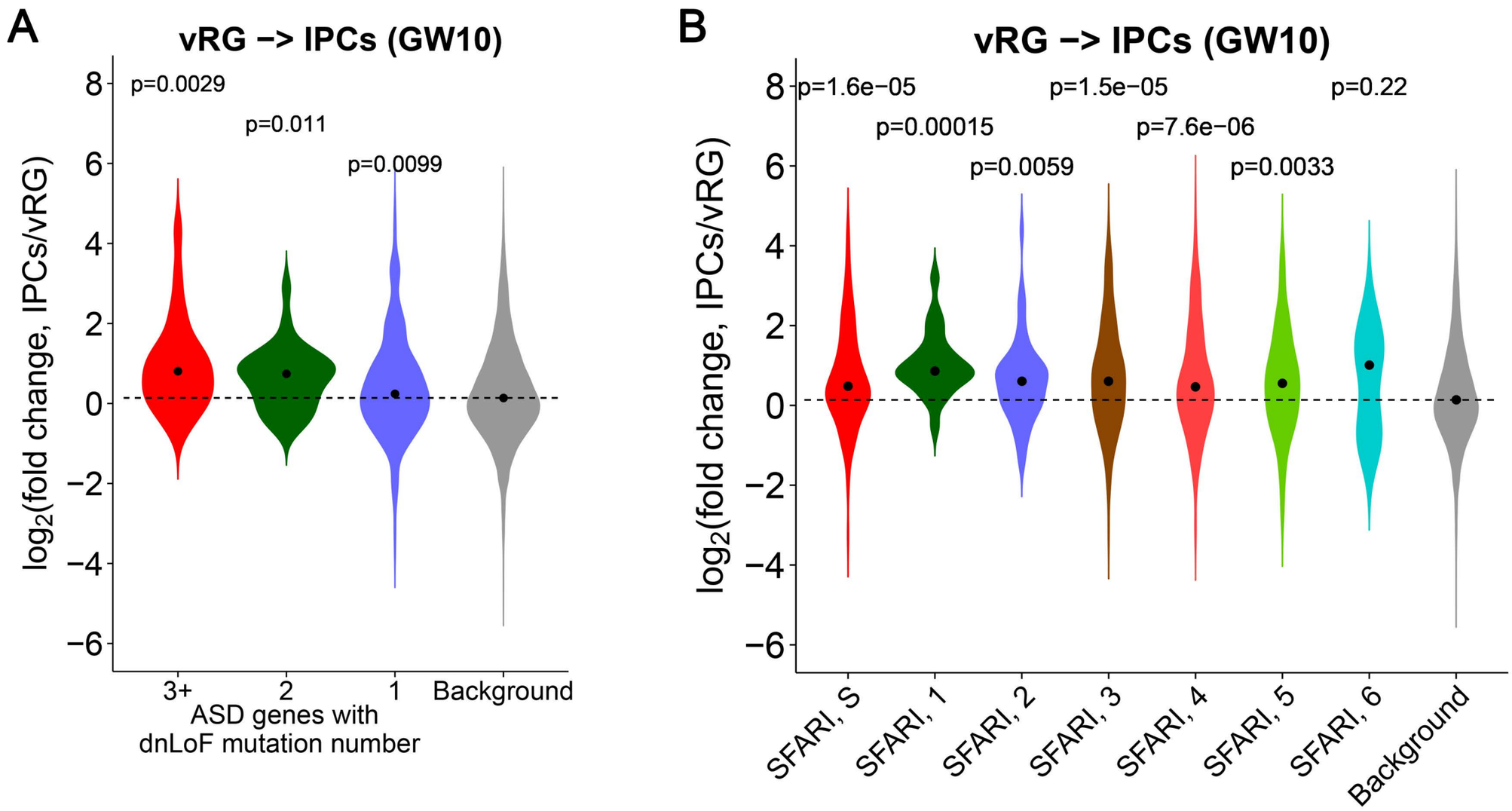

Supplemental Figure S22. Expression change of diverse ASD gene sets during the transition from vRG cells to IPCs at GW10. (*A*) Expression change of ASD genes with ≥3, 2 and 1 dnLoF mutations during the transition. Dashed horizontal line indicates the median $\log_2$(fold change) value of the background genes. P values indicate whether different types of ASD genes with dnLoF mutations have higher $\log_2$(fold change) values than the background genes (one-sided Wilcoxon rank-sum test). (*B*) Expression change of different types of SFARI ASD genes during the transition. Dashed horizontal line indicates the median $\log_2$(fold change) value of the background genes. P values indicate whether different types of SFARI ASD genes have higher $\log_2$(fold change) values than the background genes (one-sided Wilcoxon rank-sum test).

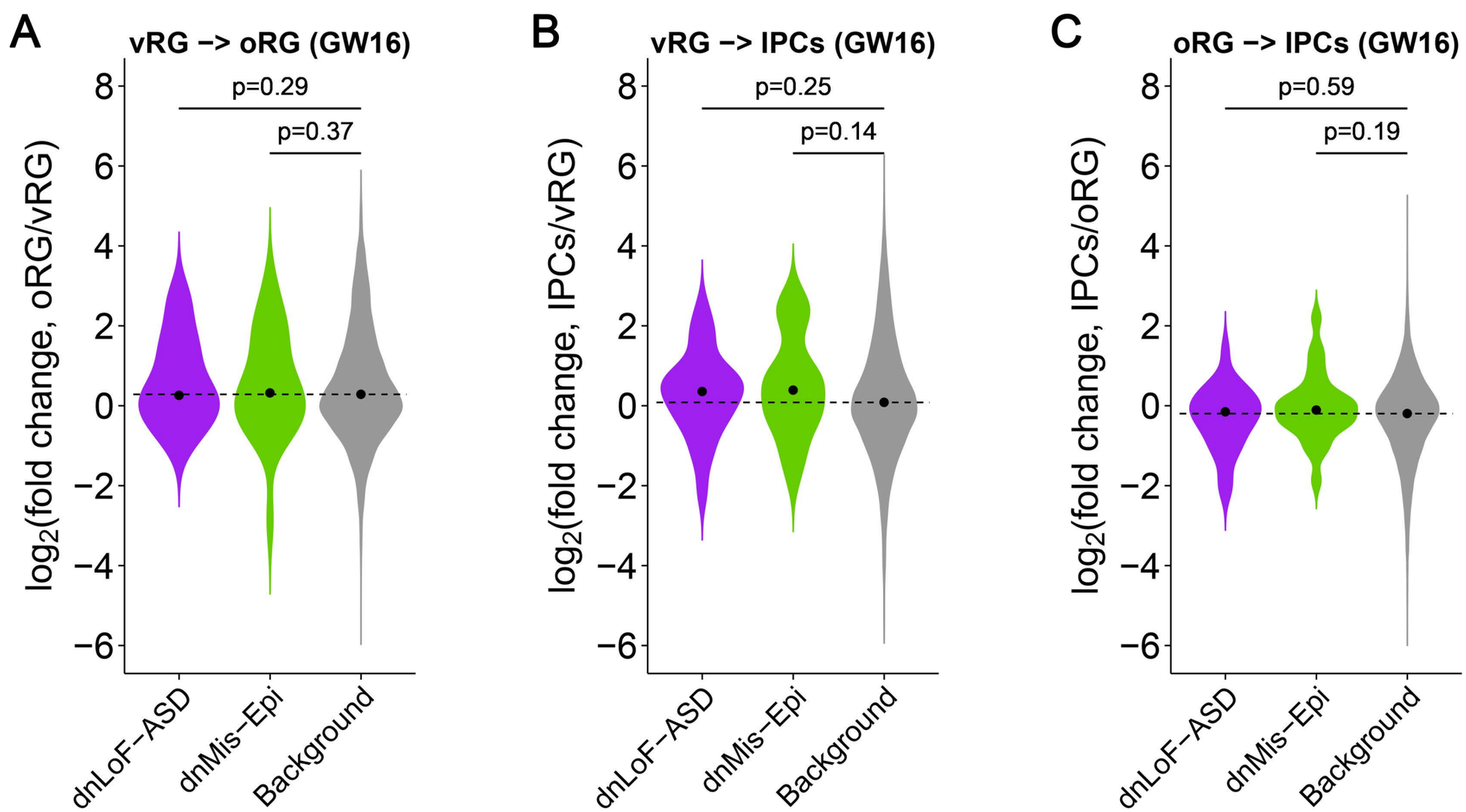

Supplemental Figure S23. Expression change of dnLoF-ASD and dnMis-Epi genes during the cell type transitions within NPCs at GW16. (*A*-*C*) Expression change of dnLoF-ASD and dnMis-Epi genes during the transitions at GW16 from vRG cells to oRG cells (*A*), vRG cells to IPCs (*B*), and oRG cells to IPCs (*C*). Dashed horizontal line indicates the median $\log_2$(fold change) value of the background genes. P values indicate whether dnLoF-ASD and dnMis-Epi genes have higher $\log_2$(fold change) values than the background genes during the transitions (one-sided Wilcoxon rank-sum test).

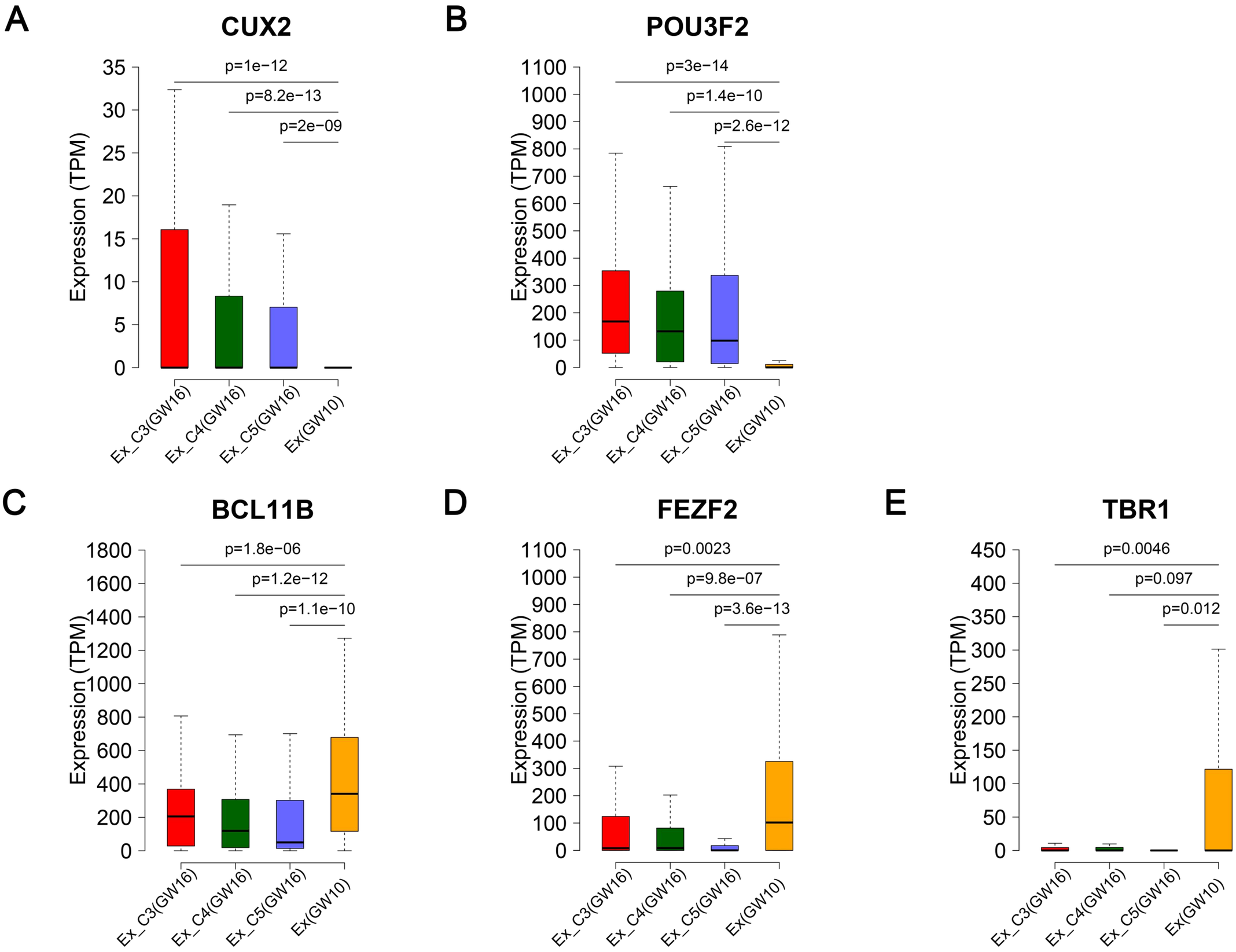

Supplemental Figure S24. Expression difference of layer marker genes in subclusters of excitatory neurons (Ex) at GW16 compared with excitatory neurons at GW10. (*A-E*) Expression difference of upper-layer neuron markers *CUX2* (*A*), and *POU3F2* (*B*), and deep-layer neuron markers *BCL11B* (*C*), *FEZF2* (*D*), and *TBR1* (*E*) in the three subclusters of excitatory neurons at GW16 compared with excitatory neurons at GW10. P values indicate expression difference of layer marker genes between GW16 excitatory neuron subclusters and GW10 excitatory neurons using DESeq2.

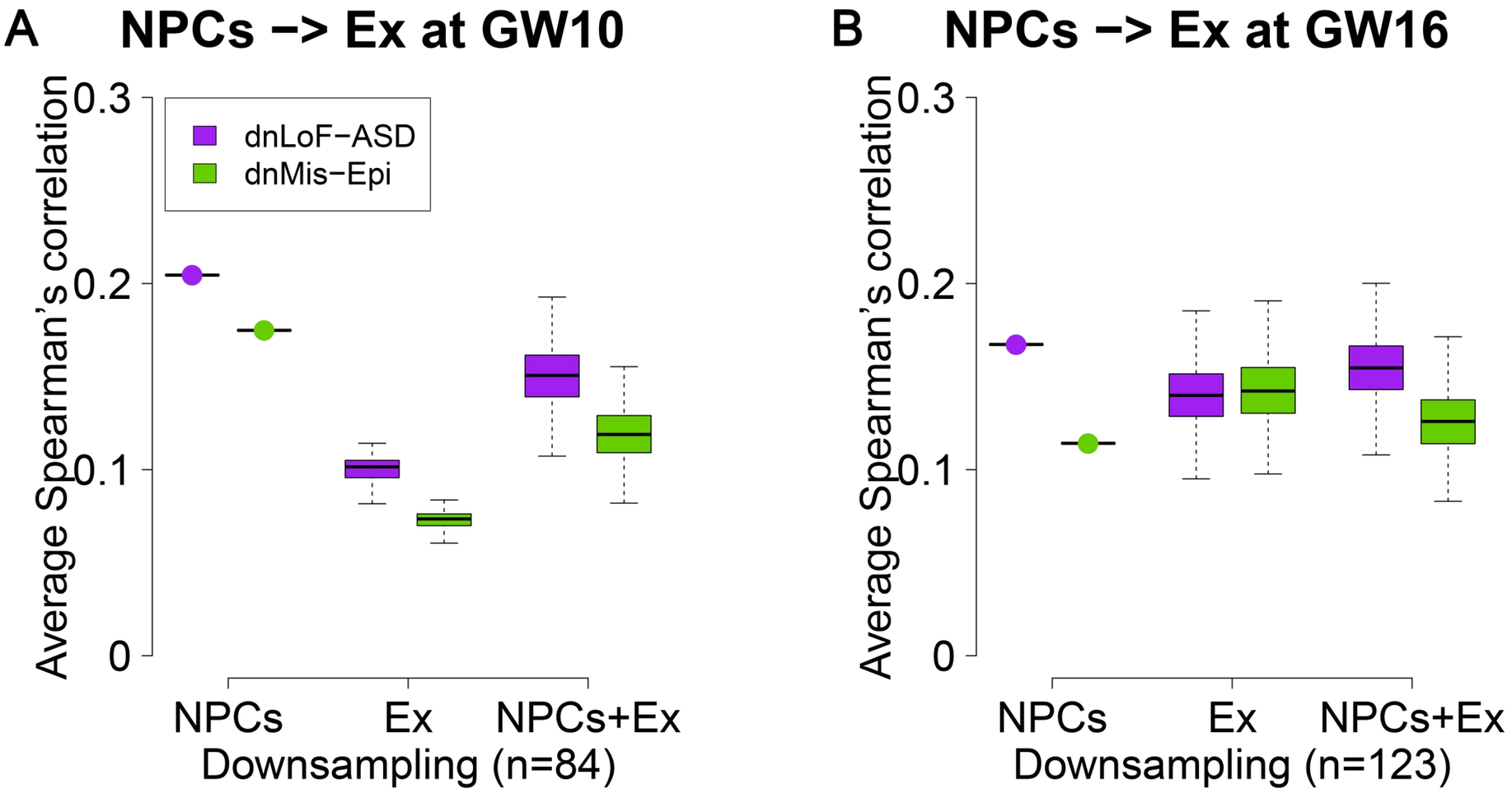

Supplemental Figure S25. Spearman's correlation analysis of dnLoF-ASD and dnMis-Epi genes during differentiation from NPCs to excitatory neurons (Ex) by downsampling. (*A,B*) Average Spearman's correlation of dnLoF-ASD and dnMis-Epi genes in NPCs, excitatory neurons, and the differentiation at GW10 (*A*) and GW16 (*B*) by downsampling the same number of cells for each condition.

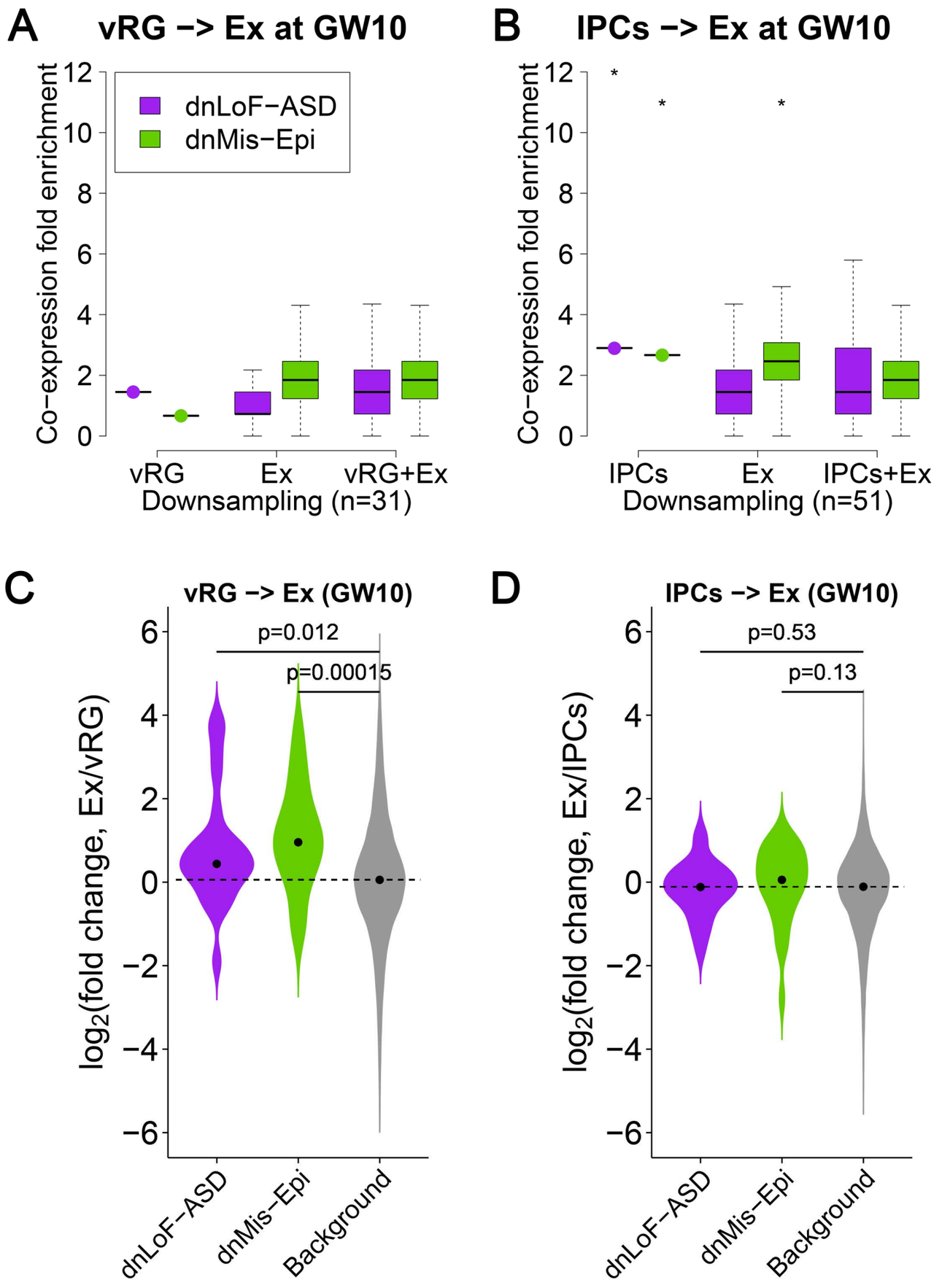

Supplemental Figure S26. Co-expression enrichment analysis of dnLoF-ASD and dnMis-Epi genes during the differentiation from vRG cells and IPCs to excitatory neurons (Ex) at GW10. (*A,B*) Co-expression fold enrichment of dnLoF-ASD and dnMis-Epi genes in vRG cells, excitatory neurons, and the differentiation at GW10 (*A*) and in IPCs, excitatory neurons, and the differentiation at GW10 (*B*) by downsampling the same number of cells for each condition. Asterisks indicate -$\log_{10}$P values for differences in mean enrichment scores between the gene sets and the background genes (one-sided Fisher's exact test): * 1≤ -$\log_{10}$P <2; ** 2≤ -$\log_{10}$P <5; *** 5≤ -$\log_{10}$P <10; **** 10≤ -$\log_{10}$P. (*C,D*) Expression change of dnLoF-ASD and dnMis-Epi genes during the differentiation at GW10 from vRG cells to excitatory neurons (*C*) and IPCs to excitatory neurons (*D*). Dashed horizontal line indicates the median $\log_2$(fold change) value of the background genes. P values indicate whether dnLoF-ASD and dnMis-Epi genes have higher $\log_2$(fold change) values than the background genes during the differentiation (one-sided Wilcoxon rank-sum test).

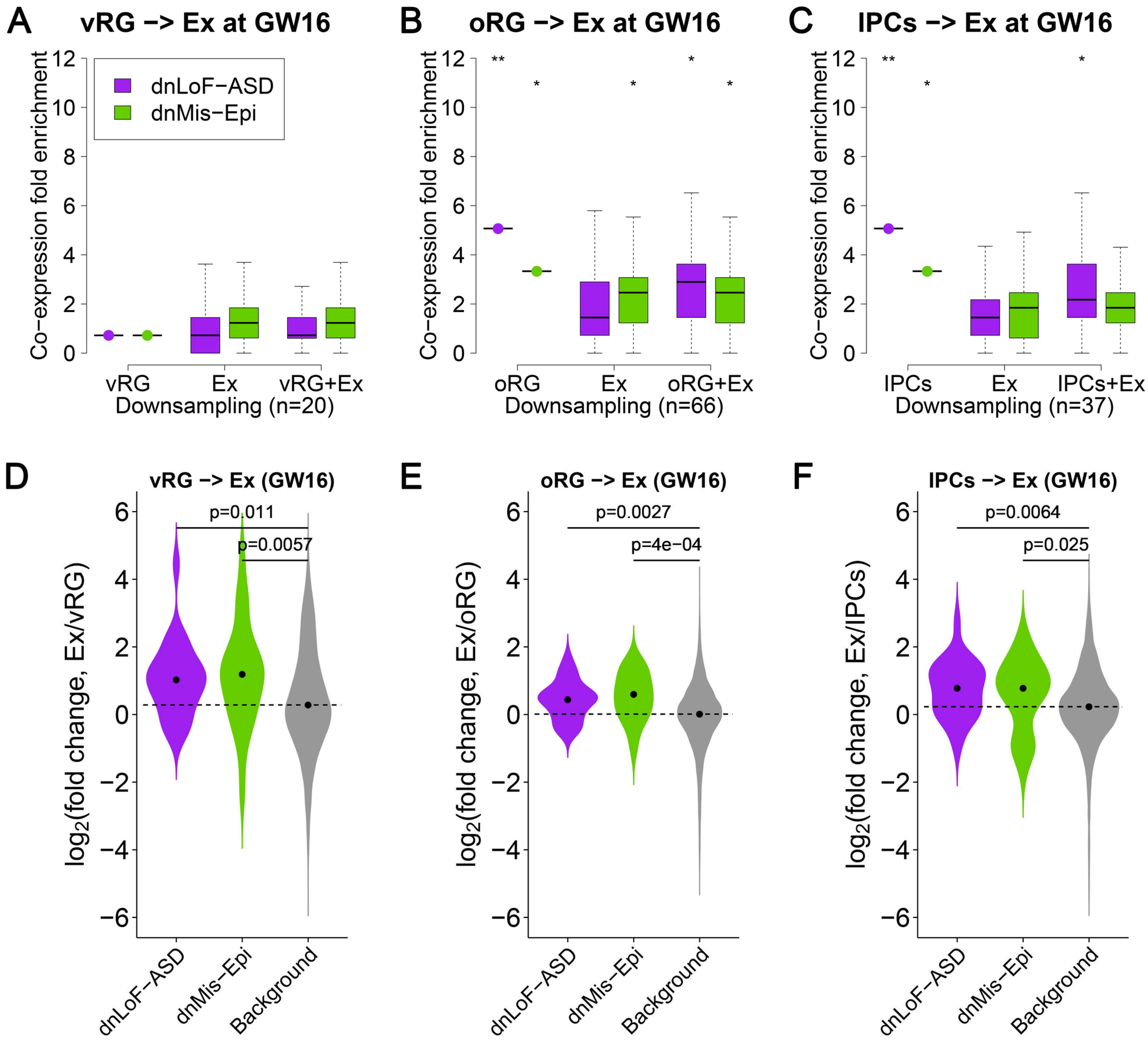

Supplemental Figure S27. Co-expression enrichment analysis of dnLoF-ASD and dnMis-Epi genes during the differentiation from vRG cells, oRG cells, and IPCs to excitatory neurons (Ex) at GW16. (*A-C*) Co-expression fold enrichment of dnLoF-ASD and dnMis-Epi genes in vRG cells, excitatory neurons, and the differentiation at GW16 (*A*), in oRG cells, excitatory neurons, and the differentiation at GW16 (*B*), and in IPCs, excitatory neurons, and the differentiation at GW16 (*C*) by downsampling the same number of cells for each condition. Asterisks indicate -$\log_{10}$P values for differences in mean enrichment scores between the gene sets and the background genes (one-sided Fisher's exact test): * 1≤ -$\log_{10}$P <2; ** 2≤ -$\log_{10}$P <5; *** 5≤ -$\log_{10}$P <10; **** 10≤ -$\log_{10}$P. (*D-F*) Expression change of dnLoF-ASD and dnMis-Epi genes during the differentiation at GW16 from vRG cells to excitatory neurons (*D*), oRG cells to excitatory neurons (*E*), and IPCs to excitatory neurons (*F*). Dashed horizontal line indicates the median $\log_2$(fold change) value of the background genes. P values indicate whether dnLoF-ASD and dnMis-Epi genes have higher $\log_2$(fold change) values than the background genes during the differentiation (one-sided Wilcoxon rank-sum test).

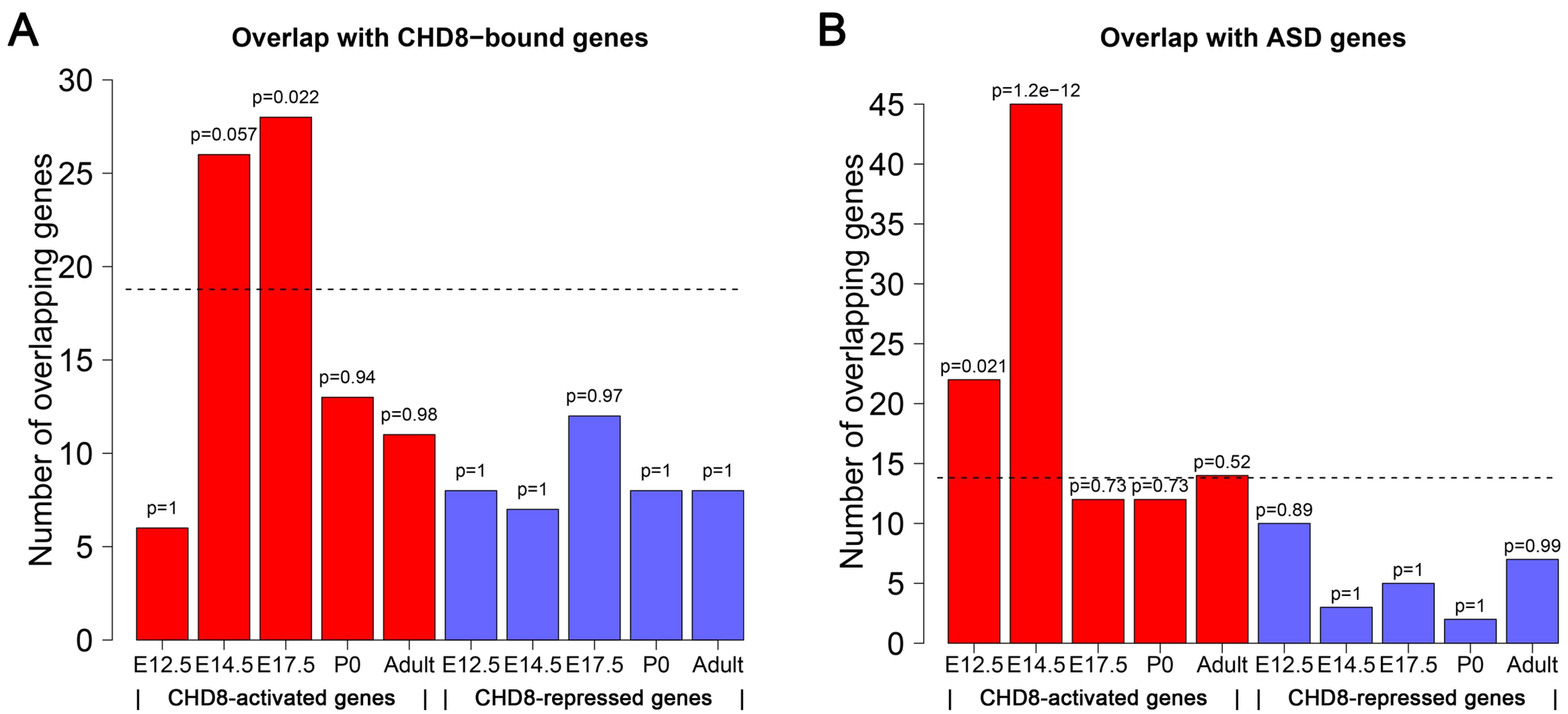

Supplemental Figure S28. *CHD8* target gene selection. (*A*) Overlap between *CHD8*-activated/-repressed genes and *CHD8*-bound genes. Dashed horizontal line indicates the expected number of *CHD8*-bound genes among 300 random genes from the background genes. P values indicate whether *CHD8*-activated and -repressed genes are enriched with *CHD8*-bound genes (one-sided Fisher's exact test). (*B*) Overlap between *CHD8*-activated/-repressed genes and ASD genes with at least one dnLoF mutation. Dashed horizontal line indicates the expected number of ASD genes among 300 random genes from the background genes. P values indicate whether *CHD8*-activated and -repressed genes are enriched with ASD genes (one-sided Fisher's exact test).